Check for updates

Coupled Carbonate Chemistry - Harmful Algae Bloom Models for Studying Effects of Ocean Acidification on *Prorocentrum minimum* Blooms in a Eutrophic Estuary

Renjian Li [*], Ming Li and Patricia M. Glibert

Horn Point Laboratory, University of Maryland Center for Environment Science, Cambridge, MD, United States

Eutrophic estuaries have suffered from a proliferation of harmful algal blooms (HABs) and acceleration of ocean acidification (OA) over the past few decades. Despite laboratory experiments indicating pH effects on algal growth, little is understood about how acidification affects HABs in estuaries that typically feature strong horizontal and vertical gradients in pH and other carbonate chemistry parameters. Here, coupled hydrodynamic–carbonate chemistry–HAB models were developed to gain a better understanding of OA effects on a high biomass HAB in a eutrophic estuary and to project how the global anthropogenic CO_2 increase might affect these HABs in the future climate. *Prorocentrum minimum* in Chesapeake bay, USA, one of the most common HAB species in estuarine waters, was used as an example for studying the OA effects on HABs. Laboratory data on *P. minimum* grown under different pH conditions were applied in the development of an empirical formula relating growth rate to pH. Hindcast simulation using the coupled hydrodynamic-carbonate chemistry–HAB models showed that the *P. minimum* blooms were enhanced in the upper bay where pH was low. On the other hand, pH effects on *P. minimum* growth in the mid and lower bay with higher pH were minimal, but model simulations show surface seaward estuarine flow exported the higher biomass in the upper bay downstream. Future model projections with higher atmospheric pCO_2 show that the bay-wide averaged *P. minimum* concentration during the bloom periods increases by 2.9% in 2050 and 6.2% in 2100 as pH decreases and 0.2 or 0.4, respectively. Overall the model results suggest OA will cause a moderate amplification of *P. minimum* blooms in Chesapeake bay. The coupled modeling framework developed here can be applied to study the effects of OA on other HAB species in estuarine and coastal environments.

Keywords: harmful algal bloom, *Prorocentrum minimum*, ocean acidification, pH, climate change, numerical model, Chesapeake bay

INTRODUCTION

The frequency, duration, and intensity of harmful algal blooms (HABs) have increased due to eutrophication as well as global climate change in recent decades (Glibert and Burford, 2017; Glibert, 2020). Climate change is impacting HABs in complex ways, from warming of waters, to changing precipitation patterns and changing stratification (Paerl and Huisman, 2008; Wells et al., 2015; Glibert, 2020). Ocean acidification (OA), a consequence of oceanic uptake of excess atmospheric CO_2, could also contribute to the global expansion of HABs, but its effects on HABs are not as well understood as other climate change factors.

CO_2 enrichment is expected to relieve the energy requirements of photosynthesis, especially of those primary producers that rely on carbon concentrating mechanisms (CCMs) to overcome inorganic C limitation. CCMs increase the concentration of CO_2 at the site of Rubisco, the primary carboxylating enzyme in photosynthesis. In particular, those species having Form II Rubisco, which has a lower affinity for CO_2 than form I, would be expected to benefit when CO_2 is enriched (Tortell, 2000; Rost et al., 2003; Giordano et al., 2005; Raven and Beardall, 2014). Many bloom-forming dinoflagellates fall into this category and rising CO_2 could stimulate the growth of these species. In addition to impacting C fixation, decreasing pH also could influence algal growth by affecting nutrient uptake. Lowered pH could affect nutrient acquisition by altering the cellular transmembrane potential, enzyme activity (Beardall and Raven, 2004; Giordano et al., 2005), or chemical speciation of dissolved nutrients (Shi et al., 2010). Despite the varied effects of increasing CO_2 on dinoflagellates and their complex physiological responses, limited previous studies suggested that OA could stimulate the growth of many HAB species (e.g. Beardall et al., 2009; O'Neil et al., 2012; Wells et al., 2015; Glibert, 2020).

During the past half-century, levels of atmospheric and surface water CO_2 concentrations have increased by more than 25%, lowering pH in the ocean by about 0.1 unit (Doney et al., 2012; Takahashi et al., 2014; Bates et al., 2014; Doney et al., 2020). Surface water pH of the ocean is expected to decrease further by 0.3 – 0.4 unit by the end of the 21st century (Feely et al., 2004; Feely et al., 2009; Jiang et al., 2019; IPCC, 2021). Compared with the open ocean, coastal and large estuaries are experiencing an accelerated pace of acidification, as organic matter respiration contributes to dissolved inorganic C production, in addition to CO_2 uptake from the atmosphere (Cai et al., 2011; Cai et al., 2017; Cai et al., 2021). Therefore, eutrophication exerts a dual effect on estuaries and coastal oceans, not only stimulating HABs but also exacerbating OA. Chesapeake bay, the largest estuary in the U.S., which suffers from both OA and HABs, provides an excellent system to investigate the impacts of OA on HAB abundance and distribution.

Recent observations in Chesapeake bay found pH and surface pCO_2 to have large spatial gradients and strong temporal variabilities (Brodeur et al., 2019; Huang et al., 2019; Shadwick et al., 2019; Chen et al., 2020; Friedman et al., 2020). The pH range is large, with a minimum value of 7.1 in the upper bay and

the bottom waters of the mid bay and a maximum value as high as 8.5 in the surface waters of the mid and lower bay (Brodeur et al., 2019). pCO_2 also displays a strong along-channel gradient from the estuary's head to mouth, resulting in outgassing in the upper bay, uptake of atmospheric CO_2 in the mid bay, and near-equilibrium conditions in the lower bay (Cai et al., 2017; Chen et al., 2020; Friedman et al., 2020). Observations from a moored sensor showed high frequency fluctuations of pH and pCO_2, driven by a wide array of physical and biological processes (Shadwick et al., 2019).

Modeling studies and retrospective data analysis have shown significant but complex long-term pH trends in Chesapeake bay over the past three decades (Shen et al., 2020; Da et al., 2021). In the upper bay, where pH in near-surface waters has historically been low, there has been a long-term increase (basification), influenced by freshwater input and increasing alkalinity in the Susquehanna River (Kaushal et al., 2013). In contrast, in the lower bay, which historically had a higher pH, there has been a decrease in pH and acidification due to oceanic influence. Due to the counter-balance between OA and river alkalinization (Shen et al., 2020), pH in the autotrophic mid-bay has shown no significant long term trends but displays strong short-term fluctuations likely associated with phytoplankton photosynthesis. Also, seasonally, calcium carbonate dissolution is an important buffering mechanism for pH changes in late summer in the mid-bay, leading to higher pH values in August than in June, despite persistent hypoxic conditions during the summer (Su et al., 2020; Su et al., 2021). How these long term pH trends and seasonal variations affect seasonal development of HABs and how the increasing atmospheric pCO_2 in a warming climate influence HABs are largely unknown but are of critical importance for managing coastal resources.

Prorocentrum minimum, a species of increasing global concern (Heil et al., 2005; Glibert et al., 2008; Glibert et al., 2012), is one of the major bloom-forming harmful dinoflagellates of Chesapeake bay. Blooms of *P. minimum* can lead to hypoxic events, death of finfish and shellfish, and submerged aquatic vegetation losses (Tango et al., 2005). Such blooms are restricted to certain ranges of temperature and salinity, and occur most frequently in April and May (Tango et al., 2005; Li et al., 2015). Bloom events of this species have increased from ~13 per year in the 1990s to > 20 per year in the early 2000s in Chesapeake bay (Li et al., 2015). However, the effects of pH on *P. minimum* growth have been seldom investigated although there were some laboratory experimental studies. Under high pH, growth of *P. minimum* is greatly reduced, while its growth rate increases moderately as pH decreases (Hansen, 2002). Fu et al. (2008) found CO_2 enrichment could increase the growth rate of *P. minimum* by increasing its maximum light-saturated C fixation rate. Later experiments found extremely low pH (< 7) could also limit growth of dinoflagellates, but *P. minimum* was able to survive under such conditions (Berge et al., 2010). These laboratories studies were conducted with *P. minimum* under fixed values of pH or CO_2 concentration. It remains unclear how *P. minimum* is affected by varying pH level *in situ* in an estuarine environment as it is transported in the estuary and its position

varies seasonally (Tyler and Seliger, 1978; Zhang et al., 2021; Li et al., 2021). A mechanistic model that integrates hydrodynamics, carbonate chemistry and harmful algae physiology is needed to address such questions.

Few plankton models have explicitly incorporated the effects of pH or pCO_2 and have been mainly used to interpret results obtained from controlled laboratory experiments (e.g. Schippers et al., 2004; Flynn et al., 2015; Almomani, 2019). In this study we developed a new integrated modeling system to investigate the effects of OA on *P. minimum* blooms *in vivo*, by coupling 3D hydrodynamic, carbonate chemistry and HAB models. The model results provide a first glimpse into the effects of OA on HABs in a dynamic and variable present and future estuarine environment. The modeling system is based on widely used ocean models and can be readily applied to other estuaries and coastal oceans.
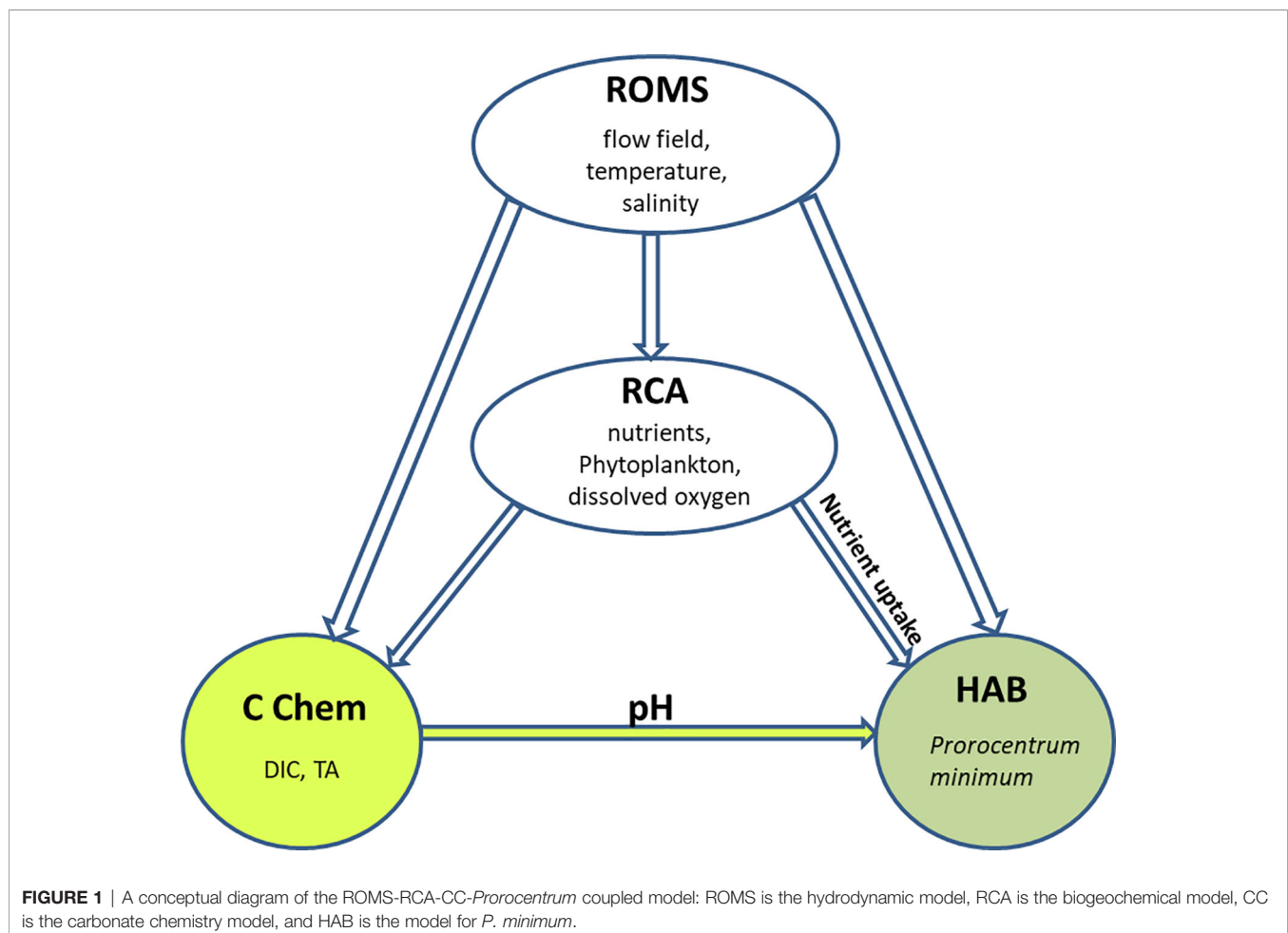
METHODS

The integrated modeling system consists of four submodels: a hydrodynamic model based on the Regional Ocean Modeling System (ROMS) (Shchepetk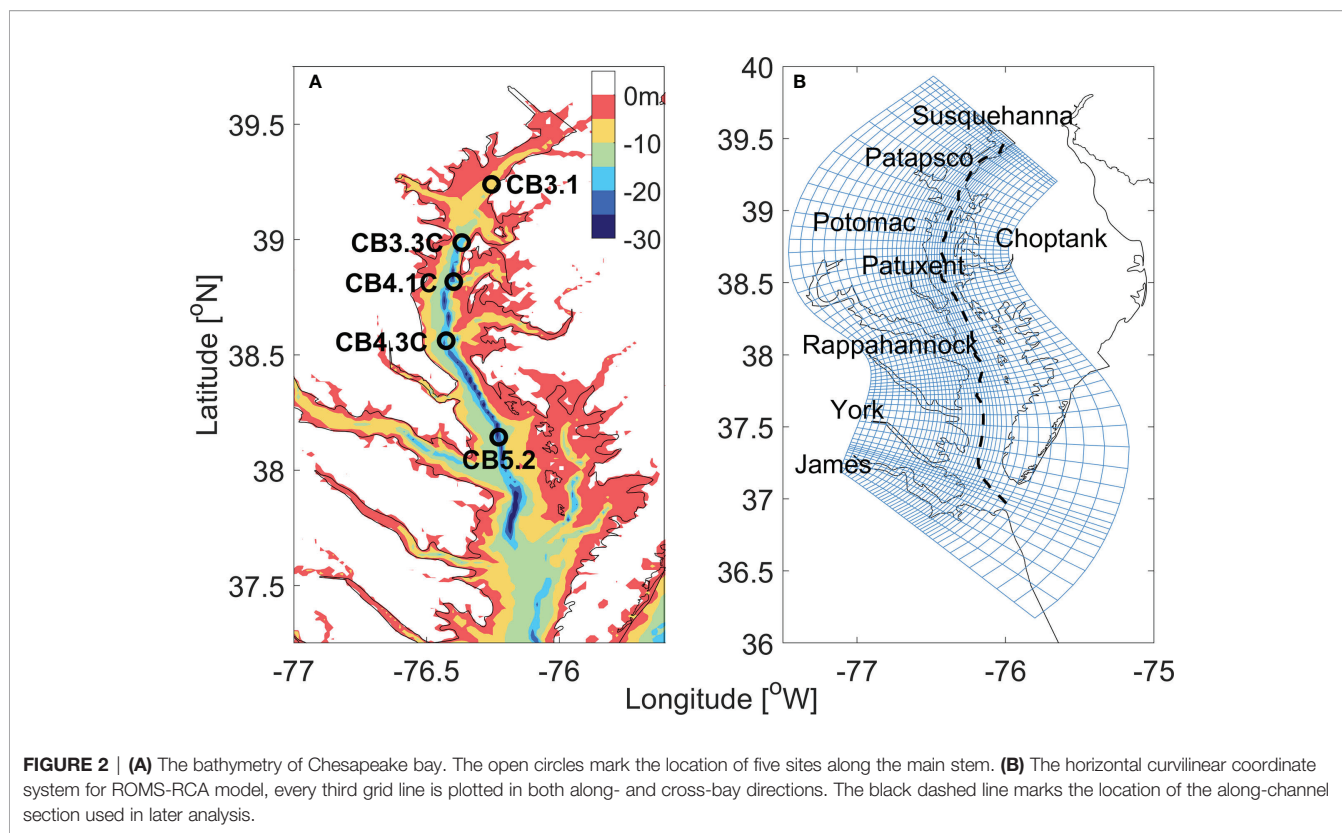in and McWilliams, 2005; Haidvogel et al., 2008); a biogeochemical model based on the Row Column Aesop (RCA) structure (Di Toro, 2001; Isleib et al., 2007; Testa et al., 2014); a carbonate chemistry (CC) model based on Shen et al. (2019a); and a HAB model based on a mechanistic model developed by Zhang et al. (2021). This integrated modeling system is termed ROMS-RCA-CC-*Prorocentrum* (**Figure 1**).

Hydrodynamic Model (ROMS)

The ROMS hydrodynamic model was configured for Chesapeake bay and its adjacent shelf (**Figure 2**), consisting of 80 × 120 grid points in the horizontal direction and 20 evenly distributed vertical sigma levels in the vertical direction (Li et al., 2005). An orthogonal curvilinear coordinate system was used to follow the general orientation of the deep channel and the coastlines of the main stem of the bay. Coastal boundaries were specified as a finite-discretized grid *via* land/sea masking.

ROMS is forced by freshwater discharge at river heads, water levels at the open boundary, and heat and momentum flux across the sea surface. The freshwater input was prescribed for the eight major tributaries of Chesapeake bay, based on measurements at US Geological Survey gaging stations (USGS). The offshore boundary water level consists of tidal and non-tidal components. The tidal component was provided by global tidal

FIGURE 1 | A conceptual diagram of the ROMS-RCA-CC-*Prorocentrum* coupled model: ROMS is the hydrodynamic model, RCA is the biogeochemical model, CC is the carbonate chemistry model, and HAB is the model for *P. minimum*.

FIGURE 2 | **(A)** The bathymetry of Chesapeake bay. The open circles mark the location of five sites along the main stem. **(B)** The horizontal curvilinear coordinate system for ROMS-RCA model, every third grid line is plotted in both along- and cross-bay directions. The black dashed line marks the location of the along-channel section used in later analysis.

model TPXO7 (TOPEX/POSEIDON) (Egbert and Erofeeva, 2002), and the non-tidal component was extracted from daily sea level measured at Duck, North Carolina, by the National Oceanic and Atmospheric Administration (NOAA). The air-sea heat flux and momentum flux were computed by using the North America Regional Reanalysis (NARR) data. The vertical eddy viscosity and diffusivity were parameterized using the k-kl turbulence closure scheme with the background value of $1 \times 10^{-6} \text{ m}^2 \text{ s}^{-1}$, and the horizontal eddy viscosity and diffusivity were set to be constant ($1 \text{ m}^2 \text{ s}^{-1}$). The ROMS model was initialized using climatological temperature and salinity conditions and run for a spin-up period of 2 years to get the initial condition for year 2006. A detailed description of the model configuration can be found in Li et al. (2005). This hydrodynamic model was previously validated against water level measurements at tidal gauge stations (Zhong and Li, 2006; Zhong et al., 2008), salinity and temperature time series at monitoring stations (Li et al., 2005; Ni et al., 2020), salinity distributions collected during hydrographic surveys, and current measurements (Li et al., 2005; Xie and Li, 2018; Xie and Li, 2019), including the year of 2006 (Ni et al., 2020).

Biogeochemical Model (RCA)
The RCA biogeochemical model includes a water-column component (Isleib et al., 2007) and a sediment diagenesis component (Di Toro, 2001), coupled to the ROMS hydrodynamic model in an offline mode. RCA simulates pools of organic and inorganic nutrients, two phytoplankton groups

(one representing winter-spring diatoms and one representing summer dinoflagellates), and dissolved oxygen concentrations (Testa et al., 2014). The RCA biogeochemical model is forced by loads of dissolved and particulate materials from the eight major rivers. Riverine constituent concentrations for phytoplankton, silica, particulate and dissolved organic C, phosphorus (P), and nitrogen (N), and inorganic nutrients $[\text{NH}_4^+, \text{NO}_2^- + \text{NO}_3^-$ hereafter $\text{NO}_3^-, \text{PO}_4^{3-}]$ were obtained or derived from Chesapeake bay Program biweekly monitoring data as described in Testa et al. (2014). The ocean boundary concentrations were acquired from the World Ocean Atlas 2013 and Filippino et al. (2011). Atmospheric deposition of nutrients was much smaller than the riverine nutrient loading and thus not considered, following the previous studies (Ni et al., 2020; Li et al., 2020b; Zhang et al., 2021). The initial conditions of RCA were based on Chesapeake bay Program monitoring data in December 2005. The RCA model has been validated against biogeochemical data at a number of stations in Chesapeake bay (including NO_3^-, PO_4^{3-}, NH_4^+, chlorophyll-a, dissolved oxygen, and organic C, N and P), integrated metrics of hypoxic volume, rates of water-column primary production and respiration, and nutrient fluxes across the sediment-water surface (Brady et al., 2013; Testa et al., 2013; Testa et al., 2014; Li et al., 2016; Testa et al., 2017; Ni et al., 2020).

Carbonate chemistry Model (CC)
The CC model simulates Dissolved Inorganic Carbon (DIC), Total Alkalinity (TA), and mineral calcium carbonate (aragonite CaCO_3) and has previously been coupled to ROMS-RCA for

Chesapeake bay (Shen et al., 2019a; Shen et al., 2019b; Shen et al., 2020). DIC is consumed by phytoplankton growth/photosynthesis and calcium carbonate precipitation. The sources of DIC include air-sea CO_2 flux, phytoplankton respiration, oxidation of organic matter, calcium carbonate dissolution, sulfate reduction, and sediment water fluxes. Calcium carbonate dissolution and precipitation are the primary source/sinks for TA, but the contributions of several other biogeochemical processes (e.g., nitrification and sulfate reduction) to TA are also modeled. Other carbonate chemistry parameters such as pH and pCO$_2$ are calculated from the CC model outputs using the CO2SYS program (Lewis and Wallace, 1998). A detailed description of the CC model and its coupling to RCA is described in Shen et al. (2019a). The CC model is forced by the atmospheric CO_2, the riverine loads and offshore concentration of TA and DIC. Time series of TA measurements in riverine inputs were obtained from the USGS stations in the Susquehanna and Potomac Rivers (Raymond et al., 2000). The riverine DIC concentrations were calculated through CO2SYS with the available TA and pH (Shen et al., 2020). Carbonate chemistry data for the other smaller tributaries were estimated using empirical relationships as functions of freshwater discharge (Shen et al., 2019a). TA at the ocean boundary was directly estimated with the empirical equation based upon salinity at the ocean boundary (Cai et al., 2010). DIC at the offshore boundary was calculated with the available TA, fCO$_2$ from SOCAT (Bakker et al., 2016), salinity and temperature using CO2SYS. The atmosphere pCO$_2$ was set to be 400 ppm in 2006, a year chosen for historical validation, according to the observation from NOAA-ESRL (https://www.esrl.noaa.gov/gmd/ccgg/trends; Li et al., 2020a). Initial conditions for DIC and TA were calculated from the two-end member mixing model. The CC model has been validated against extensive surveys of DIC, TA and pH collected during ten cruises in 2016 (Shen et al., 2019a) and long term (1985-2015) measurements of pH at a number of monitoring stations (Shen et al., 2019b; Shen et al., 2020).

P. minimum Model (HAB) Incorporating pH Effects

The *P. minimum* model is a mechanistic HAB model that has previously been embedded within RCA for Chesapeake bay (Zhang et al., 2021). A rhomboid strategy was used: that is, *P. minimum* is modeled individually while the two other plankton populations (winter diatoms and summer dinoflagellates) are represented by the aggregate functional classes. The model parameters for *P. minimum* are given in Zhang et al. (2021) and the parameters for the winter-spring diatoms and summer dinoflagellates can be found in Testa et al. (2014).

For the *P. minimum* model, the growth rate depends on temperature, light and nutrient concentrations, while the mortality terms include both grazing and respiration, and the model parameters have been calibrated according to published physiological experiments on *P. minimum* and numerical sensitivity-analysis experiments. The equation for *P. minimum* biomass is given by

$$\frac{d(proro)}{dt} = G * proro - R_{res} * proro - R_{gz} * proro^2 \qquad (1)$$

where *proro* is the biomass of *P. minimum* measured by carbon (in unit of mgC L^{-1}), G is the growth rate, R_{res} is the respiration rate, and R_{gz} is the grazing rate. To include the effects of pH on *P. minimum* growth, G is calculated as

$$G = G_T * G_{par} * G_N * G_{pH} \qquad (2)$$

where G_T is the specific growth rate depending on temperature, G_{par} represents the effects of light availability, G_N represents the effects of nutrient limitation on growth, and G_{pH} represents the effects of pH on growth. The formulae for G_T, G_{par} and G_N can be found in Zhang et al. (2021). In Eq. (2) G_T and G_{pH} were assumed to be independent of each other, but some previous laboratory experiments showed that elevated CO_2 alone led to a higher growth rate but elevated CO_2 in concert with temperature increase had no significant effect on *P. minimum* growth (Fu et al., 2008). Equation (2) can be readily modified to consider nonlinear interactions between higher CO_2 and warming when more experimental data are available.

G_{pH} was estimated by fitting an empirical relation to previously published experimental data on *P. minimum* culture grown under different pH conditions (Hansen, 2002; Berge et al., 2010; **Figure 3**). In those experiments, *P. minimum* growth rates were obtained in a laboratory setting under a range of pH conditions while other parameters such as temperature and salinity were held at fixed values. To capture the sole effect of pH on the growth rate, G_{pH} was normalized by the respective mean value in each laboratory experiment such that *P. minimum* growth is enhanced by OA when $G_{pH} > 1$ but suppressed by it when $G_{pH} < 1$. pH values in Hansen's (2002) experiments ranged
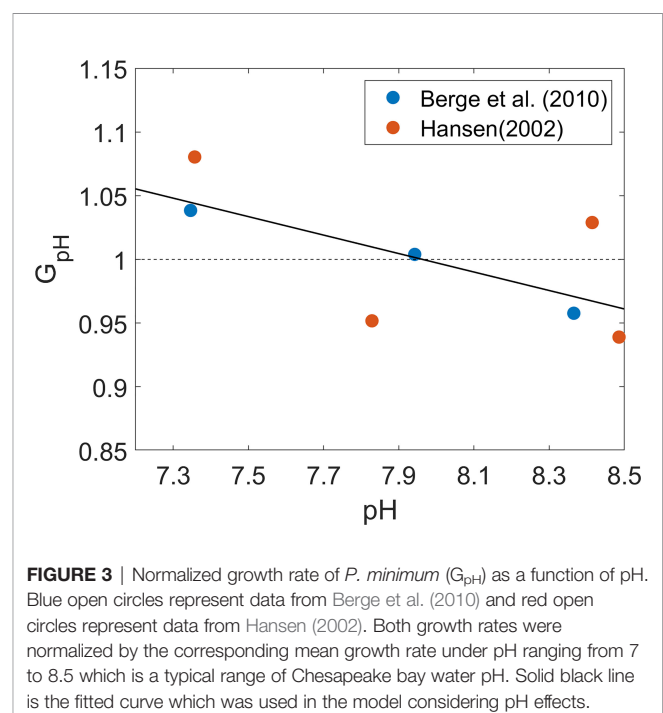

FIGURE 3 | Normalized growth rate of *P. minimum* (G_{pH}) as a function of pH. Blue open circles represent data from Berge et al. (2010) and red open circles represent data from Hansen (2002). Both growth rates were normalized by the corresponding mean growth rate under pH ranging from 7 to 8.5 which is a typical range of Chesapeake bay water pH. Solid black line is the fitted curve which was used in the model considering pH effects.

from 7 – 10, far beyond the pH range observed in Chesapeake bay, but only experimental data in the pH range of 7.2 – 8.5 are shown in **Figure 3**. G_{pH} increased by about 10% as pH decreased from 8.5 to 7.2, representing a modest enhancement of growth rate.

The boundary conditions for *P. minimum* at the river heads and continental shelf were set to 0. The initial condition of *P. minimum* for the entire estuary were interpolated using the distribution reported in the estuary-wide surveys reported in Tyler and Seliger (1978). Model sensitivity-analysis experiments in Zhang et al. (2021) showed that the prediction of *P. minimum* blooms is insensitive to the initial condition as long as a small seed population exists at the beginning of the year.

Numerical Runs

The new coupled models were first used to conduct a hindcast simulation for the year 2006. The results were used to compare with the simulations by the original ROMS-RCA-*Prorocentrum* model which did not consider pH effects (Zhang et al., 2021).

To project the future effects of OA on *P. minimum* blooms, two climate projection runs were conducted by increasing the atmospheric pCO_2 to 550 ppm for the mid-21st century and 800 ppm for the late-21st century (IPCC, 2021) and using the corresponding DIC at the oceanic boundary to drive the CC model. The oceanic boundary DIC was calculated by assuming that the pCO_2 difference between the atmosphere and the ocean surface is the same as year 2006. The initial DIC conditions for two projection runs were calculated from the two-end member mixing model with the new oceanic end DIC. Other boundary and initial conditions as well as hydrodynamic forcings were assumed to be unchanged.

RESULTS

Temporal and Spatial Patterns in pH Effects on *P. minimum* Bloom

To show the effects of OA on *P. minimum* blooms, the time series of the daily surface pH, G_{pH} and *P. minimum* biomass concentration at four stations along the Chesapeake bay mainstem (their locations marked in **Figure 2A**) are presented for the year of 2006 and the model runs with or without considering pH effects are compared.

At the upper bay station CB3.1, surface pH increased from ~7.5 to ~7.9 from winter to early spring (**Figure 4A**). It then decreased from the middle of April and reached a minimum (~7.0) in August, before recovering to higher values during the fall. Since pH at the upper bay station was relatively low, $G_{pH} > 1$ all year, yielding ~5% amplification in the modeled growth rate (**Figure 4B**). Accordingly, the *P. minimum* concentrations in the model run incorporating pH effects were moderately higher than those without considering pH effects (**Figure 4C**). The peak concentration in May reached 1.18×10^6 cells L^{-1} in the model run with pH effects, as compared to 1.13×10^6 cells L^{-1} in the model run without pH effects. This represented a 5-10% increase

in the biomass during the primary May bloom (**Figure 4D**), although larger increases (up to 20%) were seen in the fall season during which a smaller bloom developed. At station CB3.3C further downstream, the Seasonal variation of surface pH was similar to station CB3.1 except pH increased dramatically to 8.5 in June (**Figure 4E**). Though the surface pH was about 0.15 larger, G_{pH} was still above 1 during the bloom period (**Figure 4F**). The peak concentration increased by 0.05×10^6 cells L^{-1} (**Figure 4G**), representing a 3-5% increase in the bloom size (**Figure 4H**). The model-predicted *P. minimum* cell density is in good agreement with the observed cell density at CB 3.3C as well as at the stations in the mid-bay (CB 4.3C) and lower-bay (CB 5.2) where the monitoring data were available (**Figures 4G, K, O**).

At the mid bay station CB4.3C, surface pH generally increased from 7.9 to 8.2 between January and July (**Figure 4I**). It then dropped and reached the minimum (~ 7.5) in August and subsequently increased from September to December. The corresponding G_{pH} was slightly >1 during most of the time from January to May and then decreased to <1 in June and July (**Figure 4J**). G_{pH} increased to >1 in August and then decreased to slightly <1 again from September to December. Thus, surface *P. minimum* concentrations considering pH effects were also slightly higher than those without pH effects (**Figure 4K**), with the peak concentration during the spring bloom increasing by <5% (**Figure 4L**). At the lower bay station CB5.2, surface pH averaged around 8 and showed a weaker seasonal variation (**Figure 4M**). G_{pH} was slightly less than 1 all year except in August when pH reached the minimum (**Figure 4N**). There was virtually no difference in the cell density between the two model runs except in the late fall (**Figures 4O, P**). It was surprising to see higher *P. minimum* concentration at CB4.3C (4.2% increase) and CB5.2 (3.0% increase) during late fall when pH was high and $G_{pH} < 1$ (**Figures 4J, N**). On the other hand, *P. minimum* concentrations at the upper bay station CB3.1 remained elevated due to consistently low pH (**Figure 4D**). Seaward estuarine outflow could advect the higher biomass downstream, raising the cell density in the mid and lower bay even though the local growth rate was lower.

Focusing on the primary spring bloom period, monthly averaged surface pH in April increased from 7.7 in the upper bay to 8.0 in the mid bay while values were slightly lower, 7.9, in the lower bay (**Figure 5A**). G_{pH} was > 1 in the upper bay and < 1 in the mid-bay (**Figure 5B**). In the lower bay, G_{pH} was almost equal 1. Consequently *P. minimum* concentrations were moderately higher in the model run considering the pH effects (**Figures 5C, D**). In May, surface pH values in the mid bay and lower bay were similar to April, while the minimum surface pH in the upper bay declined to ~ 7.5 (**Figure 5E**). G_{pH} increased by 5% in the upper bay while dipping slight less than 1 in the mid-bay where pH remained above 8 (**Figure 5F**). The *P. minimum* bloom in May was mostly confined to the mid and upper bay, covering the mainstem between 38 and 39.2°N, as well as the Potomac River (**Figure 5G**). *P. minimum* concentrations increased everywhere in the bay, with the largest increase in the area between 38.7 and 39.3 °N (**Figure 5H**). The maximum increase in the cell density was 7×10^4 cells L^{-1} in the upper bay.
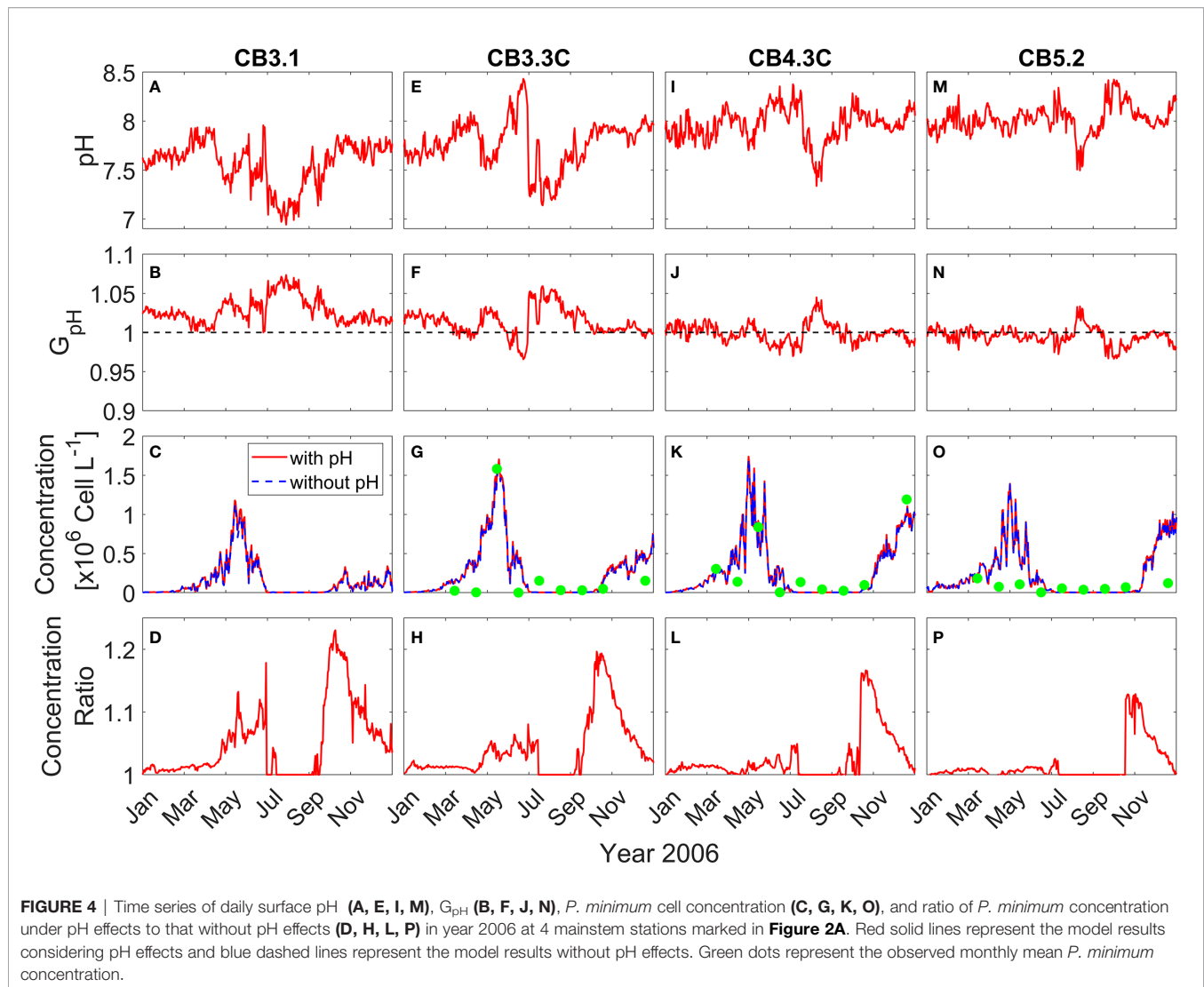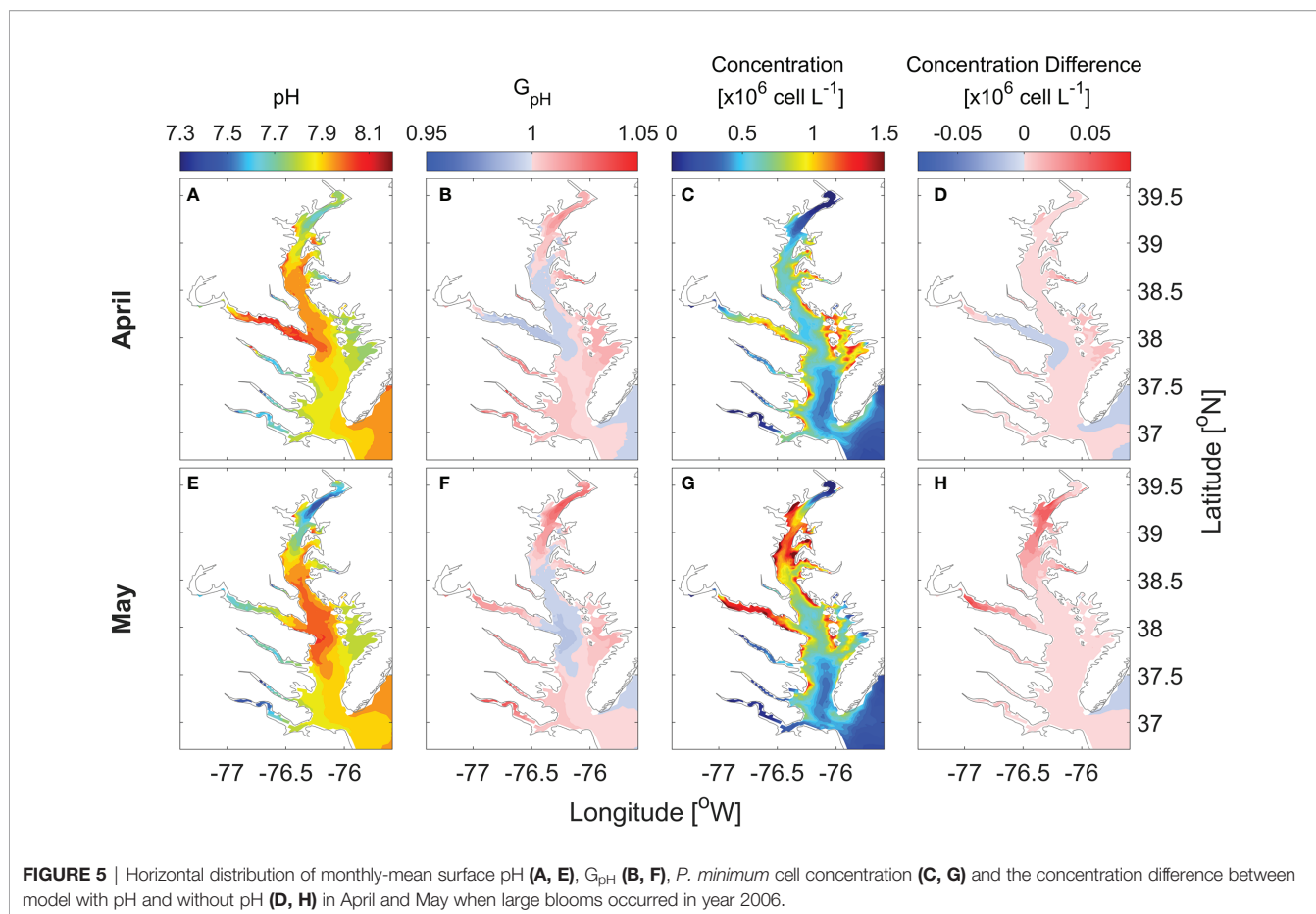
FIGURE 4 | Time series of daily surface pH **(A, E, I, M)**, G_{pH} **(B, F, J, N)**, *P. minimum* cell concentration **(C, G, K, O)**, and ratio of *P. minimum* concentration under pH effects to that without pH effects **(D, H, L, P)** in year 2006 at 4 mainstem stations marked in **Figure 2A**. Red solid lines represent the model results considering pH effects and blue dashed lines represent the model results without pH effects. Green dots represent the observed monthly mean *P. minimum* concentration.

Along-channel distributions of pH, G_{pH}, and cell concentrations provide further information on the pH effects on the cell distributions (**Figure 6**). pH showed an along-channel gradient but also a vertical gradient, with the top-to-bottom difference reaching ~0.8 in the mid-bay (**Figures 6A, E**). G_{pH} of the bottom water was >1 due to lower pH (**Figures 6B, F**). In April, *P. minimum* concentrations were highest in the bottom waters of the lower bay as cells were advected landward by the estuarine return flow (**Figure 6C**). Since *P. minimum* growth was severely limited by light availability in the bottom waters, *P. minimum* concentrations did not increase despite the lower pH values (**Figure 6D**). In May, the bloom developed in the surface waters of the mid bay and upper bay (**Figure 6G**). Low pH in the upper bay enhanced G_{pH} (**Figure 6F**) and amplified the bloom size (**Figure 6H**). Although G_{pH} < 1 in the surface waters of the mid-bay, seaward advection of higher biomass from the upper bay compensated for the lower growth rate such that the *P. minimum* concentration in the mid-bay did not decrease (**Figure 6H**).

Projections for Effects of Future Acidification on *P. minimum* Bloom

To explore the impact of OA on *P. minimum* blooms in the future climate, the time series of the daily surface pH, pH decline, G_{pH} and *P. minimum* concentrations were compared for the years 2006, mid-21st century 2050 and late-21st century 2100 at the three stations (**Figure 7**). At the upper bay station CB3.1, pH is projected to decrease by ~0.1 in 2050 and ~0.2 in 2100 (**Figures 7A, B**). Correspondingly, G_{pH} time series shift upwards by ~0.007 in 2050 and ~0.015 in 2100 (**Figure 7C**). The averaged *P. minimum* concentrations in April and May increased 2.7% by 2050 and 5.5% by 2100 (**Figure 7D**). At the mid-bay station CB4.3C, pH shows a larger reduction, decreasing by ~0.15 in 2050 and ~0.3 in 2100 (**Figures 7E, F**). G_{pH} shifts upwards and remains > 1 all year in 2100 (**Figure 7G**). The average bloom size from April to June increases 2.0% in 2050 and 5.0% in 2100 (**Figure 7H**). pH reduction at the lower bay station CB5.2 is as large as that at CB4.3C (**Figures 7I, J**). In the mid-

FIGURE 5 | Horizontal distribution of monthly-mean surface pH **(A, E)**, G_{pH} **(B, F)**, *P. minimum* cell concentration **(C, G)** and the concentration difference between model with pH and without pH **(D, H)** in April and May when large blooms occurred in year 2006.

and late-21st century, G_{pH} is projected to stay above 1 during most of the year (**Figure 7K**). *P. minimum* concentrations during the spring blooms would increase 2.7% in 2050 and 5.3% in 2100 (**Figure 7L**). The time series of the concentration ratio between future scenarios and year 2006 show the same trend at the three stations. During the spring blooms, the percentage increase in *P. minimum* concentrations reaches a maximum in April, as pH decline is relatively larger (**Figures 7B, F, G**). It should also be noted that though the percentage increase in *P. minimum* concentrations during late fall is very large, the fall blooms are much smaller than the spring blooms.

Surface distributions of monthly averaged pH, G_{pH}, and *P. minimum* concentrations in May are altered in the future scenario relative to the year 2006 (**Figure 8**). In 2050, monthly averaged surface pH in May ranges from 7.4 to 7.9, with an averaged decrease of ~ 0.1 as compared with year 2006 (**Figure 8A**). The area where G_{pH} is >1 would cover the whole bay (**Figure 8B**). Thus, *P. minimum* concentrations increase almost everywhere in the bay (**Figure 8D**). In 2100, monthly averaged surface pH in May decreases to 7.3 – 7.7 (**Figure 8E**). With such low pH, G_{pH} is even larger, reaching 1.05 in most area of the bay (**Figure 8F**). This results in even larger increases in *P. minimum* concentrations (**Figure 8H**).

Five stations were chosen to further illustrate the effects of OA on the peak bloom size of *P. minimum* (**Figure 9**). At the upper

bay station CB3.1, the peak concentration increases 1.47% in the mid-21st century and 2.86% in the late-21st century as compared with the year 2006. Stations CB3.3C, CB4.1C, and CB4.3C are located in a region (38.5 – 39 °N) where the *P. minimum* blooms typically occur (**Figure 5G**). The peak *P. minimum* concentration at these three stations is projected to increase by 1.51%, 0.87%, 2.42% in 2050 and by 2.59%, 2.68%, 4.37% in 2100, respectively. At the station CB5.2 at the lower bay, the peak *P. minimum* concentration increases by 2.04% in 2050 and 3.73% in 2100.

DISCUSSION AND CONCLUSION

Coupled hydrodynamic-carbonate chemistry–HAB models were developed to investigate the effects of OA on *P. minimum* blooms in Chesapeake bay. To our knowledge, this was the first attempt to couple 3D carbonate chemistry and HAB models for an estuarine region, representing a preliminary but an important step towards modeling and understanding the OA-HAB interactions in a changing climate. The model results showed a moderate effect of pH on *P. minimum* blooms but estuarine circulation transported *P. minimum* cells across large pH gradients in the estuary and produced unexpected changes in the bloom size across different parts of the estuary. For example,
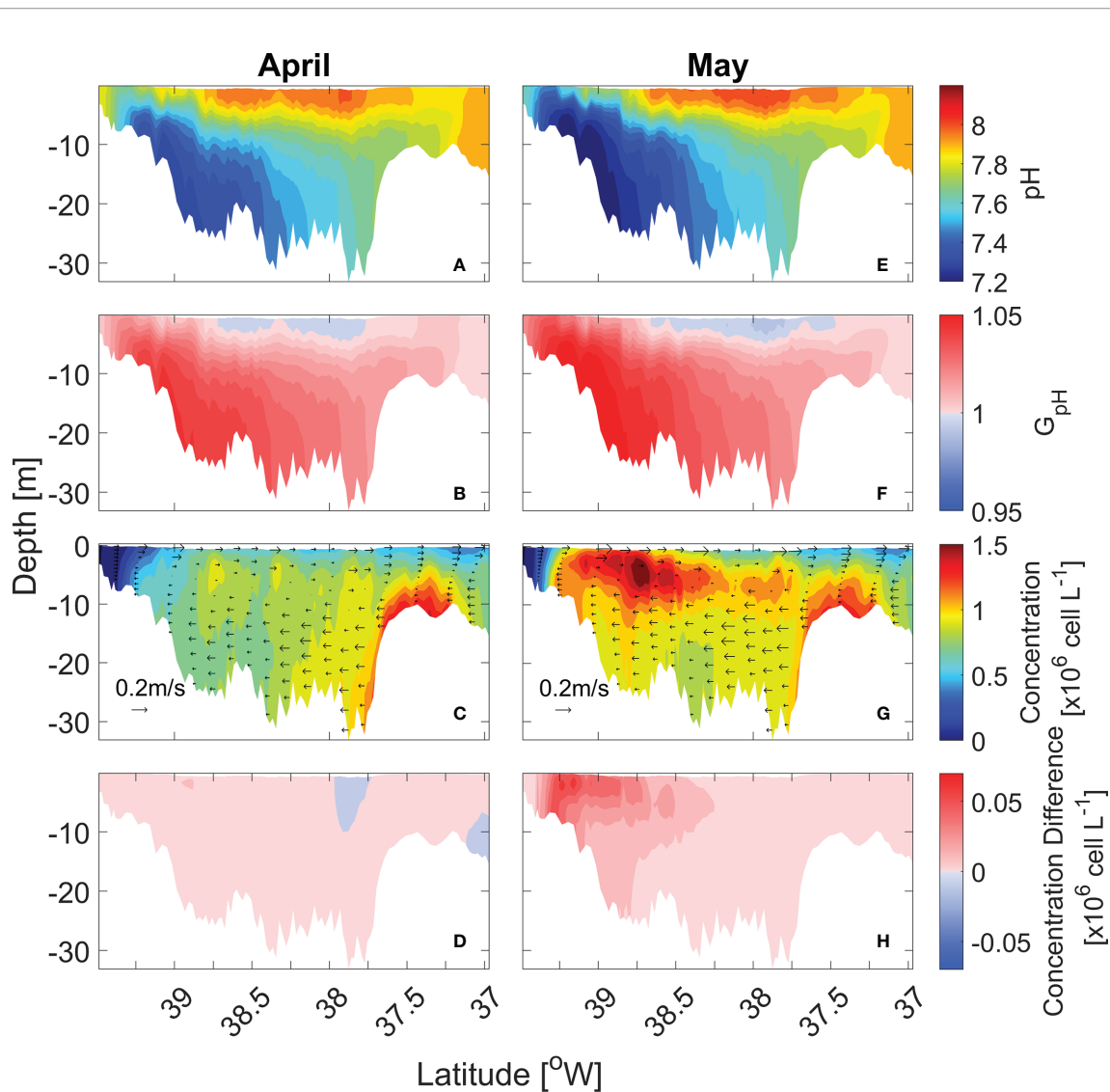
FIGURE 6 | Along-channel distribution of monthly-mean pH **(A, E)**, G_{pH} **(B, F)**, *P. minimum* cell concentration **(C, G)** and the concentration difference between model with pH and without pH **(D, H)** in April and May in year 2006.

the estuarine outflow exported higher biomass in the low-pH upper bay to the mid- and lower bay where high pH suppresses *P. minimum* growth. The climate projections suggested 2.9% or 6.2% increase in the bay-averaged *P. minimum* concentration in 2050 or 2100 when the atmospheric pCO$_2$ increases to 550 or 800 ppm and pH in Chesapeake bay decreases by 0.2 or 0.4. This modest increase is consistent with laboratory results (Fu et al., 2008; Berge et al., 2010). It is possible some phytoplankton species like *P. minimum* are resistant to climate change in terms of OA as large pH fluctuations in space and time under the current climate make them capable of tolerating OA effects. Other species may show a stronger response. A recent meta-analysis of ~3000 studies on HABs globally reveals that the effects of elevated CO$_2$ on HAB growth rates varies both across and within species, but led to a significant overall increase in growth

rate by 20% (Brandenburg et al., 2019). Our choice of *P. minimum* for this modeling study was driven by the availability of an existing mechanistic HAB model for Chesapeake bay. It is quite possible that a larger OA effect may be found for other HAB species and the modeling approach developed here can be readily extended to other HAB species in other estuaries or coastal oceans. The coupled carbonate chemistry and HAB models could also be extended to incorporate other effects of rising CO$_2$ on the HAB species as described below.

This modeling study focussed exclusively on the pH effects. However, previous studies suggested the potential effects of C limitation on algal growth under changing CO$_2$ conditions (e.g. Schippers et al., 2004; Almomani, 2019). In Chesapeake bay DIC ranges between 1000 and 2000 µM L^{-1} under the current climate
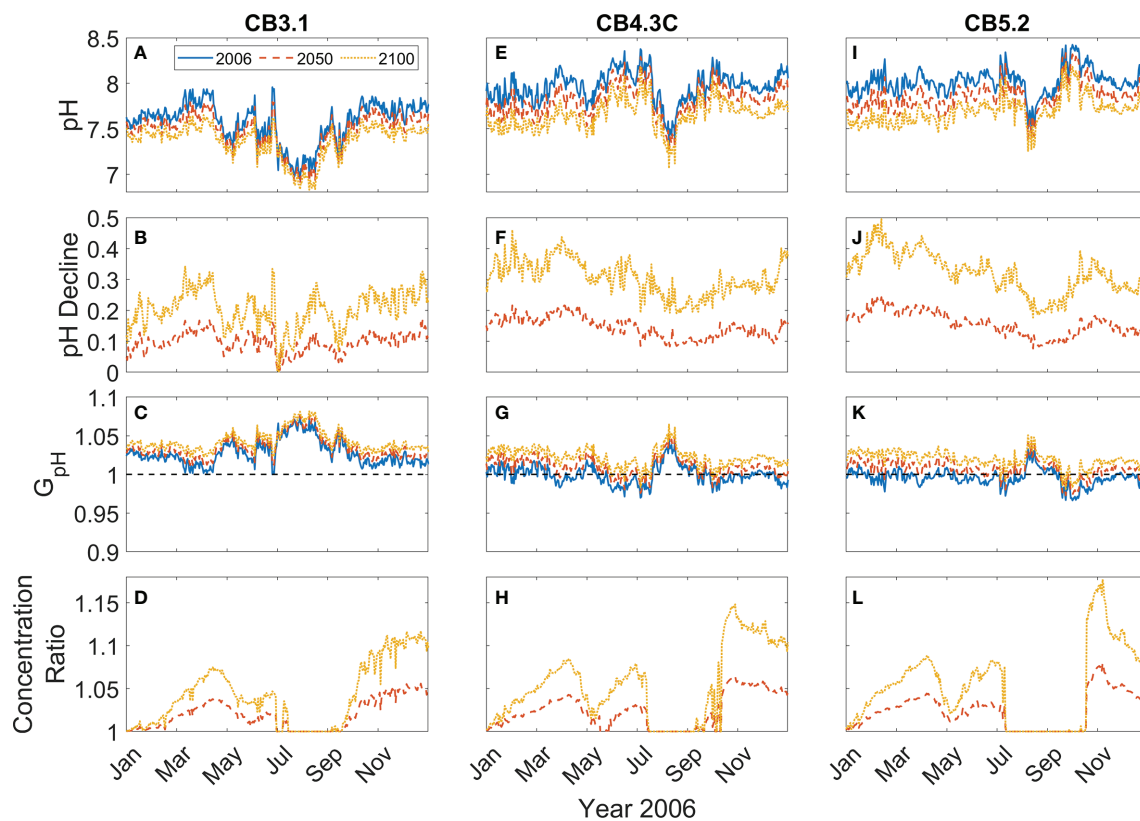
FIGURE 7 | Time series of daily surface pH **(A, E, I)**, pH decline **(B, F, J)**, GpH **(C, G, K)**, and ratio of P. minimum concentration in mid-21st century and late-21st century to that in year 2006 **(D, H, L)** at 3 mainstem stations marked in **Figure 2A**..

(Brodeur et al., 2019) and is expected to increase by 100-400 µM L^{-1} in the 21st century. Hence C limitation is not expected to be a major factor in *P. minimum* growth. Nevertheless, laboratory experiments showed that growth of species such as *P. minimum* may be affected by pH changes even when DIC limitation was minor (Hansen et al., 2007). The physiological responses of dinoflagellates to pH and CO_2 changes are likely complicated and future models need to take these processes into consideration. For example, elevated CO_2 could affect cellular quotas of C, N and P and the uptake rate of nutrients (Xia and Gao, 2005; Fu et al., 2007; Finkel et al., 2010). An increase of C:N or C:P could make the algae more prone to N-limitation or P-limitation, although elevated CO_2 did not significantly affect the elemental ratios of *P. minimum* (Fu et al., 2008).

The parameterization G$_{PH}$ used in the HAB model (Eq. 2) was based on the laboratory experiments in which pH in the culture was altered through acid/base additions. Two approaches have been used to manipulate pH and the carbonate system in studies involving phytoplankton and responses to lowered pH and OA. One is based on acid/base additions and the other is CO_2 bubbling. The main difference lies in their different effects on the carbonate speciation, the total pool of inorganic C (TCO$_2$), and alkalinity of seawater medium (Berge et al., 2010). CO_2 bubbling leads to an increase in TCO$_2$ while alkalinity is kept

constant and pH decreases. This reflects the changes related to ocean acidification due to increased atmospheric CO_2. In the HCl addition method, TCO$_2$ is kept stable while total alkalinity and pH decrease. There are heated discussions on which technique is most suitable for studying OA effects (Hurd et al., 2009; Schulz et al., 2009; Shi et al., 2009). The pros and cons of each technique make it more difficult to evaluate effects in estuarine and coastal environments where there are multiple sources of inorganic C (e.g. riverine inputs, oceanic import, uptake from the atmosphere, respiration of organic matter). Future modeling development for studying OA-HAB interaction requires a close integration between the experimental and modeling approaches.

To investigate the influence of future acidification on *P. minimum* blooms, two scenario runs were conducted under the elevated pCO$_2$ conditions projected for the mid- and late-21st century conditions. However, these model runs did not consider all climate-change impacts on Chesapeake bay such as warming, sea level rise and altered river flows (Ni et al., 2019). In their laboratory experiments, Fu et al. (2008) found raising CO_2 alone increased the growth rate of *P. minimum* but higher CO_2 and warming in combination did not produce significant change on *P. minimum* growth. A future modeling study needs to consider these combined effects (e.g., Glibert, 2020). Previous projections
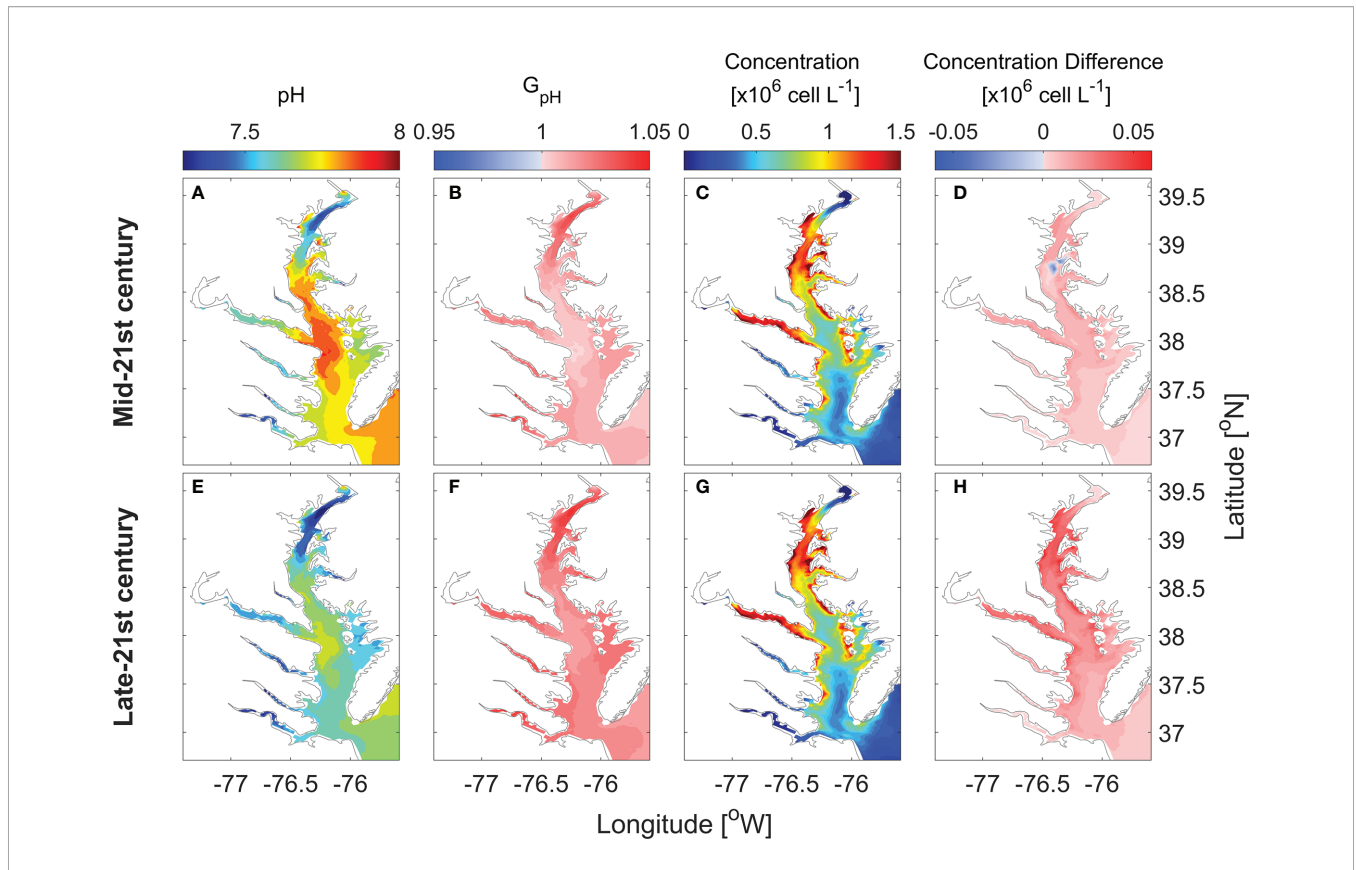
FIGURE 8 | Horizontal distribution of monthly-mean surface pH **(A, E)**, G_{pH} **(B, F)**, *P. minimum* cell concentration **(C, G)**, and the concentration difference between model results of future projection and year 2006 **(D, H)** in May.
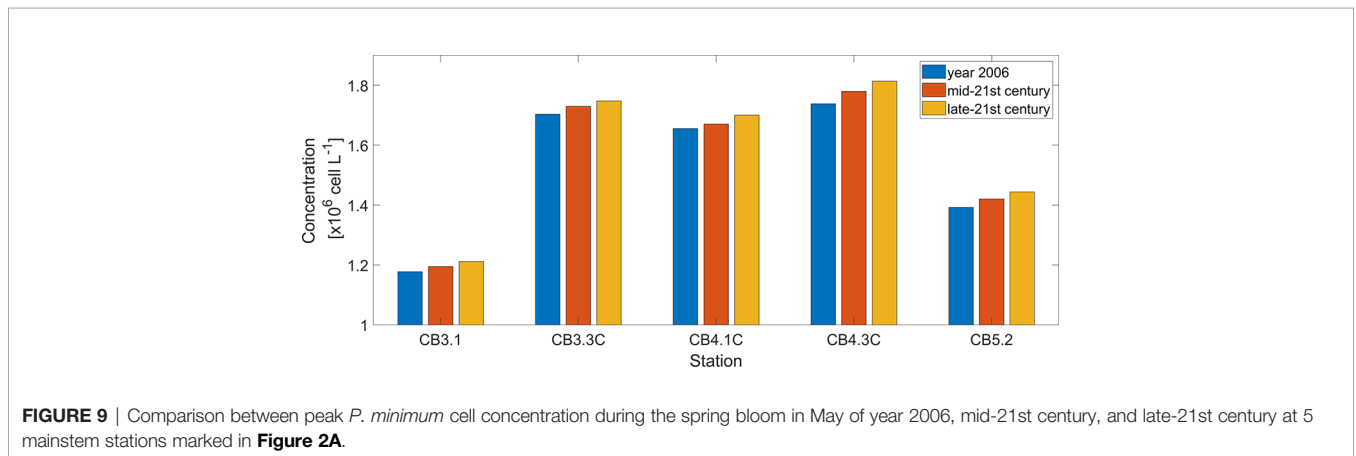

FIGURE 9 | Comparison between peak *P. minimum* cell concentration during the spring bloom in May of year 2006, mid-21st century, and late-21st century at 5 mainstem stations marked in **Figure 2A**.

of *P. minimum* in Chesapeake bay, based on a habitat model, showed that *P. minimum* biomass may shift upstream due to salinity changes caused by sea level rise and changes in the river flow (Li et al., 2020b). As the biomass in the upper bay increases, the low-pH water there may lead to a larger increase in *P. minimum* concentration and the estuarine outflow may transport these cells downstream. Furthermore, reduced pH could increase the toxicity of some harmful algae (Sun et al.,

2011; Tatters et al., 2012). While the toxicity of *P. minimum* in Chesapeake bay has not been documented, and the toxicity of this species is a topic of debate (Heil et al., 2005), the harm to estuarine ecology could be much larger under elevated pCO$_2$ for related toxic HAB taxa.

It is also worth noting that this model does not consider the complexity of mixotrophic nutrition of *P. minimum* and how that may change under altered CO$_2$ conditions. Indeed, for this

first effort of coupling the carbon chemistry model with the HAB model, a species that does not have strong dependence on mixotrophy was purposely chosen. A three-dimensional mixotrophic model for a different HAB taxon of Chesapeake bay, *Karlodinium veneficum*, has recently been developed (Li et al., 2022), and the aim is to couple this complex HAB model to the ROMS-RCA-CC model in the future.

DATA AVAILABILITY STATEMENT

Model results in this study can be downloaded from https://zenodo.org/record/6318647#.Yh274OjMKUk.

AUTHOR CONTRIBUTIONS

ML, PG, and RL conceived the ideas. RL configured the model and conducted the numerical simulations. RL and ML analyzed the model results. RL wrote the paper with editorial contributions from ML and PG. All authors contributed to the article and approved the submitted version.

REFERENCES

Almomani, F. A. (2019). Assessment and Modeling of Microalgae Growth Considering the Effects OF CO_2, Nutrients, Dissolved Organic Carbon and Solar Irradiation. *J.Env. Manage.* 247, 738–748. doi: 10.1016/j.jenvman.2019.06.085

Bakker, D. C. E., Pfeil, B., Landa, C. S., Metzl, N., O'Brien, K. M., Olsen, A., et al. (2016). A Multi-Decade Record of High-Quality fCO_2 Data in Version 3 of the Surface Ocean CO_2 Atlas (SOCAT). *Earth Syst. Sci. Data* 8, 383–413. doi: 10.5194/essd-8-383-2016

Bates, N. R., Astor, Y., Church, M., Currie, K., Dore, J., González-Dávila, M., et al. (2014). A Time-Series View of Changing Ocean Chemistry Due to Ocean Uptake of Anthropogenic CO_2 and Ocean Acidification. *Oceanography* 27 (1), 126–141. doi: 10.5670/oceanog.2014.16

Beardall, J., and Raven, J. A. (2004). The Potential Effects of Global Climate Change on Microbial Photosynthesis, Growth and Ecology. *Phycologia* 43, 26–40. doi: 10.2216/i0031-8884-43-1-26.1

Beardall, J., Stojkovic, S., and Larsen, S. (2009). Living in a High CO_2 World: Impacts of Global Climate Change on Marine Phytoplankton. *Plant Ecol. Diver.* 2 (2), 191–205. doi: 10.1080/17550870903271363

Berge, T., Daugbjerg, N., Andersen, B. B., and Hansen, P. J. (2010). Effect of Lowered pH on Marine Phytoplankton Growth Rates. *Mar. Ecol. Prog. Ser.* 416, 79–91. doi: 10.3354/meps08780

Brady, D. C., Testa, J. M., Di Toro, D. M., Boynton, W. R., and Kemp, W. M. (2013). Sediment Flux Modeling: Calibration and Application for Coastal Systems. *Est. Coast. Shelf. Sci.* 117, 107–124. doi: 10.1016/j.ecss.2012.11.003

Brandenburg, K. M., Velthuis, M., and Van de Waal, D. B. (2019). Meta-Analysis Reveals Enhanced Growth of Marine Harmful Algae From Temperate Regions With Warming and Elevated CO_2 Levels. *Glob. Change Biol.* 25 (8), 2607–2618. doi: 10.1111/gcb.14678

Brodeur, J. R., Chen, B., Zhong, J., Xu, Y., Hussain, N., Scaboo, K. M., et al. (2019). Chesapeake bay Inorganic Carbon, Spatial Distribution and Seasonal Variability. *Front. Mar. Sci.* 6. doi: 10.3389/fmars.2019.00099

Cai, W., Feely, R. A., Testa, J. M., Li, M., Evans, W., Alin, S. R., et al. (2021). Natural and Anthropogenic Drivers of Acidification in Large Estuaries. *Annu. Rev. Mar. Sc.* 13, pp.23–pp.55. doi: 10.1146/annurev-marine-010419-011004

Cai, W., Huang, W., Luther, G. W., Pierrot, D., Li, M., Testa, J. M., et al. (2017). Redox Reactions and Weak Buffering Capacity Lead to Acidification in the Chesapeake bay. *Nat. Commun.* 8, 369. doi: 10.1038/s41467-017-00417-7

Cai, W.-J., Hu, X., Huang, W.-J., Jiang, L.-Q., Wang, Y., Peng, T. H., et al. (2010). Alkalinity Distribution in the Western North Atlantic Ocean Margins. *J. Geophys. Res. Ocean.* 115, C08014. doi: 10.1029/2009JC005482

Cai, W., Hu, X., Huang, W., Murrell, M. C., Lehrter, J. C., Lohrenz, S. E., et al. (2011). Acidification of Subsurface Coastal Waters Enhanced by Eutrophication. *Nat. Geosci.* 4, 766–770. doi: 10.1038/ngeo1297

Chen, B., Cai, W.-J., Brodeur, J. R., Hussain, N., Testa, J. M., Ni, W., et al. (2020). Seasonal and Spatial Variability in Surface pCO_2 and Air-Water CO_2 Flux in the Chesapeake bay. *Limnol. Oceanogr.* 65 (12), 3046–3065. doi: 10.1002/lno.11573

Da, F., Friedrichs, M. A., St-Laurent, P., Shadwick, E. H., Najjar, R. G., and Hinson, K. E. (2021). Mechanisms Driving Decadal Changes in the Carbonate System of a Coastal Plain Estuary. *J. Geophys. Res. Ocean.* 126 (6), e2021JC017239. doi: 10.1029/2021JC017239

Di Toro, D. M. (2001). *Sediment Flux Modeling* (New York, NY: Wiley-Interscience).

Doney, S. C., Busch, D. S., Cooley, S. R., and Kroeker, K. J. (2020). The Impacts of Ocean Acidification on Marine Ecosystems and Reliant Human Communities. *Annu. Rev. Environ. Resour.* 45, 83–112. doi: 10.1146/annurev-environ-012320-083019

Doney, S. C., Ruckelshaus, M., Duffy, J. E., Barry, J. P., Chan, F., English, C. V. A., et al. (2012). Climate Change Impacts on Marine Ecosystems. *Annu. Rev. Mar. Sc.* 4, 11–37. doi: 10.1146/annurev-marine-041911-111611

Egbert, G. D., and Erofeeva, S. Y. (2002). Efficient Inverse Modeling of Barotropic Ocean Tides. *J. Atmos. Ocean. Tech.* 19 (2), 183–204. doi: 10.1175/1520-0426(2002)019<0183:eimobo>2.0.co;2

Feely, R. A., Doney, S. C., and Cooley, S. R. (2009). Ocean Acidification: Present Conditions and Future Changes in a High CO_2 World. *Oceanography* 22 (4), 36–47. doi: 10.5670/oceanog.2009.95

Feely, R. A., Sabine, C. L., Lee, K., Berelson, W., Kleypas, J., Fabry, V. J., et al. (2004). Impact of Anthropogenic CO_2 on the $CaCO_3$ System in the Oceans. *Science* 305 (5682), 362–366. doi: 10.1126/science.1097329

Filippino, K. C., Mulholland, M. R., and Bernhardt, P. W. (2011). Nitrogen Uptake and Primary Productivity Rates in the Mid-Atlantic Bight (MAB). *Estuar. Coast. Shelf. Sci.* 91, 13–23. doi: 10.1016/j.ecss.2010.10.001

Finkel, Z. V., Beardall, J., Flynn, K. J., Quigg, A., Rees, T. A. V., and Raven, J. A. (2010). Phytoplankton in a Changing World: Cell Size and Elemental Stoichiometry. *J. Plankt. Res.* 32, 119–137. doi: 10.1093/plankt/fbp098

Flynn, K. J., Clark, D. R., Mitra, A., Fabian, H., Hansen, P. J., Glibert, P. M., et al. (2015). Ocean Acidification With (De) Eutrophication Will Alter Future Phytoplankton Growth and Succession. *Proc. R. Soc B.: Biol. Sci.* 282 (1804), 20142604. doi: 10.1098/rspb.2014.2604

Friedman, J. R., Shadwick, E. H., Friedrichs, M. A. M., Najjar, R. G., De Meo, O. A., Da, F., et al. (2020). Seasonal Variability of the CO_2 System in a Large Coastal Plain Estuary. *J. Geophys. Res. Ocean.* 125, e2019JC015609. doi: 10.1029/2019JC015609

Fu, F.-X., Warner, M., Zhang, Y., Feng, Y., and Hutchins, D. A. (2007). Effects of Increased Temperature and CO_2 on Photosynthesis, Growth and Elemental Ratios in the Marine Cyanobacteria *Synechococcus* and *Prochlorococcus*. *J. Phycol.* 43, 485–496. doi: 10.1111/j.1529-8817.2007.00355.x

Fu, F. X., Zhang, Y., Warner, M. E., Feng, Y., Sun, J., and Hutchins, D. A. (2008). A Comparison of Future Increased CO_2 and Temperature Effects on Sympatric *Heterosigma Akashiwo* and *Prorocentrum Minimum*. *Harmf. Algae*. 7 (1), 76–90. doi: 10.1016/j.hal.2007.05.006

Giordano, M., Beardall, J., and Raven, J. A. (2005). CO_2 Concentrating Mechanisms in Algae: Mechanisms, Environmental Modulation, and Evolution. *Annu. Rev. Plant Biol.* 56, 99–131. doi: 10.1146/annurev.arplant.56.032604.144052

Glibert, P. M. (2020). Harmful Algal at the Complex Nexus of Eutrophication and Climate Change. *Harmf. Algae*. 91, 101583. doi: 10.1016/j.hal.2019.03.001

Glibert, P. M., and Burford, M. A. (2017). Globally Changing Nutrient Loads and Harmful Algal Blooms: Recent Advances, New Paradigms and Continuing Challenges. *Oceanography* 30 (1), 44–55. doi: 10.5670/oceanog.2017.110

Glibert, P. M., Burkholder, J. M., and Kana, T. M. (2012). Recent Insights About Relationships Between Nutrient Availability, Forms, and Stoichiometry, and the Distribution, Ecophysiology, and Food Web Effects of Pelagic and Benthic *Prorocentrum* Species. *Harmf. Algae*. 14, 231–259. doi: 10.1016/j.hal.2011.10.023

Glibert, P. M., Mayorga, E., and Seitzinger, S. (2008). *Prorocentrum Minimum* Tracks Anthropogenic Nitrogen and Phosphorus Inputs on a Global Basis: Application of Spatially Explicit Nutrient Export Models. *Harmf. Algae*. 8 (1), 33–38. doi: 10.1016/j.hal.2008.08.023

Haidvogel, D. B., Arango, H., Budgell, W. P., Cornuelle, B. D., Curchitser, E., Di Lorenzo, E., et al. (2008). Ocean Forecasting in Terrain-Following Coordinates: Formulation and Skill Assessment of the Regional Ocean Modeling System. *J. Comput. Phys.* 227, 3595–3624. doi: 10.1016/j.jcp.2007.06.016

Hansen, P. J. (2002). Effect of High pH on the Growth and Survival of Marine Phytoplankton: Implications for Species Succession. *Aquat. Microb. Ecol.* 28, 279–288. doi: 10.3354/ame028279

Hansen, P. J., Lundholm, N., and Rost, B. (2007). Growth Limitation in Marine Red-Tide Dinoflagellates: Effects of pH Versus Inorganic Carbon Availability. *Mar. Ecol. Prog. Ser.* 334, 63–71. doi: 10.3354/meps334063

Heil, C. A., Glibert, P. M., and Fan, C. (2005). *Prorocentrum Minimum* (Pavillard) Schiller: A Review of a Harmful Algal Bloom Species of Growing Worldwide Importance. *Harmf. Algae*. 4 (3), 449–470. doi: 10.1016/j.hal.2004.08.003

Huang, W.-J., Cai, W.-J., Xie, X., and Li, M. (2019). Wind-Driven Lateral Variations of Partial Pressure of Carbon Dioxide in a Large Estuary. *J. Mar. Syst.* 195, 67–73. doi: 10.1016/j.jmarsys.2019.03.002

Hurd, C. L., Hepburn, C. D., Currie, K. I., Raven, J. A., and Hunter, K. A. (2009). Testing the Effects of Ocean Acidification on Algal Metabolism: Considerations for Experimental Designs. *J. Phycol.* 45, 1236–1251. doi: 10.1111/j.1529-8817.2009.00768.x

IPCC (2021). "Climate Change 2021: The Physical Science Basis," in *Contribution of Working Group I to the Sixth Assessment Report of the Intergovernmental Panel on Climate Change* (Cambridge, United Kingdom and New York, NY, USA: Cambridge University Press). doi: 10.1017/9781009157896

Isleib, R. P. E., Fitzpatrick, J. J., and Mueller, J. (2007). The Development of a Nitrogen Control Plan for a Highly Urbanized Tidal Embayment. *Proc. Water Environ. Feder.* 5, 296–320. doi: 10.2175/193864707786619152

Jiang, L.-Q., Carter, B. R., Feely, R. A., Lauvset, S. K., and Olsen, A. (2019). Surface Ocean pH and Buffer Capacity: Past, Present and Future. *Sci. Rep.* 9, 18624. doi: 10.1038/s41598-019-55039-4

Kaushal, S. S., Likens, G. E., Utz, R. M., Pace, M. L., Grese, M., and Yepsen, M. (2013). Increased River Alkalinization in the Eastern U.S. *Environ. Sci. Technol.* 47, 10,302–10,311. doi: 10.1021/es401046s

Lewis, E. R., and Wallace, D. W. R. (1998). *CO2SYS-Program Developed for CO_2 System Calculations* (Tennessee: Carbon Dioxide Inf. Anal. Centre).

Li, J., Glibert, P. M., and Gao, Y. (2015). Temporal and Spatial Changes in Chesapeake bay Water Quality and Relationships to *Prorocentrum Minimum, Karlodinium Veneficum*, and CyanoHAB Event, 1991–2008. *Harmf. Algae*. 42, 1–14. doi: 10.1016/j.hal.2014.11.003

Li, M., Lee, Y. J., Testa, J. M., Li, Y., Ni, W., Kemp, W. M., et al. (2016). What Drives Interannual Variability of Hypoxia in Chesapeake bay: Climate Forcing Versus Nutrient Loading? *Geophys. Res. Lett.* 43, 2127–2134. doi: 10.1002/2015GL067334

Li, M., Li, R., Cai, W.-J., Testa, J. M., and Shen, C. (2020a). Effects of Wind-Driven Lateral Upwelling on Estuarine Carbonate Chemistry. *Front. Mar. Sci* 7. doi: 10.3389/fmars.2020.588465

Li, M., Ni, W., Zhang, F., Glibert, P. M., and Lin, C.-H. (2020b). Climate-Induced Interannual Variability and Projected Change of Two Harmful Algal Bloom Taxa in Chesapeake bay. USA. *Sci. Tot. Environ.* 744, 140947. doi: 10.1016/j.scitotenv.2020.140947

Li, M., Zhang, F., and Glibert, P. M. (2021). Seasonal Life Strategy of *Prorocentrum Minimum* in Chesapeake bay, USA: Validation of the Role of Physical Transport Using a Coupled Physical–Biogeochemical–Harmful Algal Bloom Model. *Limnol. Oceanogr.* 66 (11), 3873–3886. doi: 10.1002/lno.11925

Li, M., Zhong, L., and Boicourt, W. C. (2005). Simulations of Chesapeake bay Estuary: Sensitivity to Turbulence Mixing Parameterizations and Comparison With Observations. *J. Geophys. Res. Ocean.* 110, C12004. doi: 10.1029/2004JC002585

Li, M., Zhang, F., and Glibert, P. M. (2021). Seasonal Life Strategy of *Prorocentrum Minimum* in Chesapeake bay, USA: Validation of the Role of Physical Transport Using a Coupled Physical–Biogeochemical–Harmful Algal Bloom Model. *Limnol. Oceanogr.* 66 (11), 3873–3886. doi: 10.1002/lno.11925

Li, M., Chen, Y., Zhang, F., Song, Y., Glibert, P.M., Stoecker, D.K., et al. (2022). A Three-dimensional Mixotrophic Model of Karlodinium Veneficum Blooms for a Eutrophic Estuary. *Harmf. Algae* 113, 102203. doi: 10.1016/j.hal.2022.102203

Ni, W., Li, M., Ross, A. C., and Najjar, R. G. (2019). Large Projected Decline in Dissolved Oxygen in a Eutrophic Estuary Due to Climate Change. *J. Geophys. Res. Ocean.* 124 (11), 8271–8289. doi: 10.1029/2019JC015274

Ni, W., Li, M., and Testa, J. M. (2020). Discerning Effects of Warming, Sea Level Rise and Nutrient Management on Long-Term Hypoxia Trends in Chesapeake bay. *Sci. Tot. Envir.* 737, 139717. doi: 10.1016/j.scitotenv.2020.139717

O'Neil, J. M., Davis, T. W., Burford, M. A., and Gobler, C. A. (2012). The Rise of Harmful Cyanobacteria Blooms: The Potential Roles of Eutrophication and Climate Change. *Harmf. Algae*. 14, 313–334. doi: 10.1016/j.hal.2011.10.027

Paerl, H. W., and Huisman, J. (2008). Blooms Like it Hot. *Science* 320, 57–58. doi: 10.1126/science.1155398

Raven, J. A., and Beardall, J. (2014). CO_2 Concentrating Mechanisms and Environmental Change. *Aquat. Bot.* 118, 24–37. doi: 10.1016/j.aquabot.2014.05.008

Raymond, P. A., Bauer, J. E., and Cole, J. J. (2000). Atmospheric CO_2 Evasion, Dissolved Inorganic Carbon Production, and Net Heterotrophy in the York River Estuary. *Limnol. Oceanogr.* 45, 1707–1717. doi: 10.4319/lo.2000.45.8.1707

Rost, B., Riebesell, U., Burkhardt, S., and Sultemeyer, D. (2003). Carbon Acquisition of Bloom-Forming Marine Phytoplankton. *Limnol. Oceanogr.* 48 (1), 55–67. doi: 10.4319/lo.2003.48.1.0055

Schippers, P., Lurling, M., and Scheffer, M. (2004). Increase of Atmospheric CO_2 Promotes Phytoplankton Productivity. *Ecol. Lett.* 7, 446–451. doi: 10.1111/j.1461-0248.2004.00597.x

Schulz, K. G., Barcelos e Ramos, J., Zeebe, R. E., and Riebesell, U. (2009). CO2 Perturbation Experiments: Similarities and Differences Between Dissolved Inorganic Carbon and Total Alkalinity Manipulations. *Biogeosciences* 6, 2145–2153. doi: 10.5194/bg-6-2145-2009

Shadwick, E. H., Friedrichs, M. A. M., Najjar, R. G., De Meo, O. A., Friedman, J. R., Da, F., et al. (2019). High Frequency CO_2 System Variability Over the Winter-to-Spring Transition in a Coastal Plain Estuary. *J. Geophys. Res. Ocean.* 124, 7626–7642. doi: 10.1029/2019JC015246

Shchepetkin, A. F., and McWilliams, J. C. (2005). The Regional Oceanic Modeling System (ROMS): A Split-Explicit, Free-Surface, Topography-Following-Coordinate Oceanic Model. *Ocean. Model.* 9, 347–404. doi: 10.1016/j.ocemod.2004.08.002

Shen, C., Testa, J. M., Li, M., and Cai, W.-J. (2020). Understanding Anthropogenic Impacts on pH and Aragonite Saturation State in Chesapeake bay: Insights From a 30-Year Model Study. *J. Geophys. Res. Biogeosci.* 125, e2019JG005620. doi: 10.1029/2019JG005620

Shen, C., Testa, J. M., Li, M., Cai, W.-J., Waldbusser, G. G., Ni, W., et al. (2019a). Controls on Carbonate System Dynamics in a Coastal Plain Estuary: A Modeling Study. *J. Geophys. Res. Biogeosci.* 124, 61–78. doi: 10.1029/2018JG004802

Shen, C., Testa, J. M., Ni, W., Cai, W.-J., Li, M., and Kemp, W. M. (2019b). Ecosystem Metabolism and Carbon Balance in Chesapeake bay: A 30-Year

Analysis Using a Coupled Hydrodynamic-Biogeochemical Model. *J. Geophys. Res. Ocean.* 124, 6141–6153. doi: 10.1029/2019jc015296

Shi, D., Xu, Y., Hopkinson, B. M., and Morel, F. M. M. (2010). Effect of Ocean Acidification on Iron Availability to Marine Phytoplankton. *Science* 327 (5966), 676–679. doi: 10.1126/science.1183517

Shi, D., Xu, Y., and Morel, F. M. M. (2009). Effects of the pH/pCO_2 Control Method on Medium Chemistry and Phytoplankton Growth. *Biogeosciences* 6, 1199–1207. doi: 10.5194/bg-6-1199-2009

Su, J., Cai, W. J., Brodeur, J., Chen, B., Hussain, N., Yao, Y., et al. (2020). Chesapeake bay Acidification Buffered by Spatially Decoupled Carbonate Mineral Cycling. *Nat. Geosci.* 13 (6), 441–447. doi: 10.1038/s41561-020-0584-3

Su, J., Cai, W. J., Testa, J. M., Brodeur, J. R., Chen, B., Scaboo, K. M., et al. (2021). Supply-Controlled Calcium Carbonate Dissolution Decouples the Seasonal Dissolved Oxygen and pH Minima in Chesapeake bay. *Limnol. Oceanogr.* 66 (10), 3796–3810. doi: 10.1002/lno.11919

Sun, J., Hutchins, D. A., Feng, Y. Y., Seubert, E. L., Caron, D. A., and Fu, F. X. (2011). Effects of Changing pCO_2 and Phosphate Availability on Domoic Acid Production and Physiology of the Marine Harmful Bloom Diatom. *Pseudo-nitzschia. Multiseries. Limnol. Oceanogr.* 56 (3), 829–840. doi: 10.4319/lo.2011.56.3.0829

Takahashi, T., Sutherland, S. C., Chipman, D. W., Goddard, J. G., Ho, C., Newberger, T., et al. (2014). Climatological Distributions of Ph, pCO_2, Total CO_2, Alkalinity, and $CaCO_3$ Saturation in the Global Surface Ocean, and Temporal Changes at Selected Locations. *Mar. Chem.* 164, 95–125. doi: 10.1016/j.marchem.2014.06.004

Tango, P. J., Magnien, R., Butler, W., Luckett, C., Luckenbach, M., Lacouture, R., et al. (2005). Impacts and Potential Effects Due to *Prorocentrum minimum* Blooms in Chesapeake bay. *Harmf. Algae.* 4, 525–531. doi: 10.1016/j.hal.2004.08.014

Tatters, A. O., Fu, F. X., and Hutchins, D. A. (2012). High CO_2 and Silicate Limitation Synergistically Increase the Toxicity of *Pseudo-Nitzshia Fraudulenta. PloS One* 7 (2), e32116. doi: 10.1371/journal.pone.0032116

Testa, J. M., Brady, D. C., Di Toro, D. M., Boynton, W. R., Cornwell, J. C., and Kemp, W. M. (2013). Sediment Flux Modeling: Nitrogen, Phosphorus and Silica Cycles. *Estuar. Coast. Shelf. Sci.* 131, 245–263. doi: 10.1016/j.ecss.2013.06.014

Testa, J. M., Li, Y., Lee, Y. J., Li, M., Brady, D. C., Di, D. M., et al. (2014). Quantifying the Effects of Nutrient Loading on Dissolved O_2 Cycling and Hypoxia in Chesapeake bay Using a Coupled Hydrodynamic – Biogeochemical Model. *J. Mar. Syst.* 139, 139–158. doi: 10.1016/j.jmarsys.2014.05.018

Testa, J. M., Li, Y., Lee, Y. J., Li, M., Brady, D. C., DiToro, D. M., et al. (2017). "Modeling Physical and Biogeochemical Controls on Dissolved Oxygen in Chesapeake bay: Lessons Learned From Simple and Complex Approaches," in *Modeling Coastal Hypoxia - Numerical Simulations of Patterns, Controls and Effects of Dissolved Oxygen Dynamics.* Eds. D. Justic, K. Rose, R. Hetland and K. Fennel (Switzerland: Springer), 95–118. doi: 10.1007/978-3-319-54571-4_5

Tortell, P. D. (2000). Evolutionary and Ecological Perspectives on Carbon Acquisition in Phytoplankton. *Limnol. Oceanogr.* 45 (3), 744–750. doi: 10.4319/lo.2000.45.3.0744

Tyler, M. A., and Seliger, H. H. (1978). Annual Subsurface Transport of a Red Tide Dinoflagellate to its Bloom Area: Water Circulation Patterns and Organism Distributions in the Chesapeake bay 1. *Limnol. Oceanogr.* 23 (2), pp.227–pp.246. doi: 10.4319/lo.1978.23.2.0227

Wells, M. L., Trainer, V. L., Smayda, T. J., Karlson, B. S., Trick, C. G., Kudela, R. M., et al. (2015). Harmful Algal Blooms and Climate Change: Learning From the Past and Present to Forecast the Future. *Harmf. Algae.* 49, 68–93. doi: 10.1016/j.hal.2015.07.009

Xia, J.-R., and Gao, K.-S. (2005). Impacts of Elevated CO_2 Concentration on Biochemical Composition, Carbonic Anhydrase, and Nitrate Reductase Activity of Freshwater Green Algae. *J. Int. Plant Biol.* 47, 668–675. doi: 10.1111/j.1744-7909.2005.00114.x

Xie, X., and Li, M. (2018). Effects of Wind Straining on Estuarine Stratification: A Combined Observational and Modeling Study. *J. Geophys. Res. Ocean.* 123, 2363–2380. doi: 10.1002/2017JC013470

Xie, X., and Li, M. (2019). Generation of Internal Lee Waves by Lateral Circulation in a Coastal Plain Estuary. *J. Phys. Oceanogr.* 49 (7), 1687–1697. doi: 10.1175/JPO-D-18-0142.1

Zhang, F., Li, M., Glibert, P. M., and Ahn, S. H. S. (2021). A Three-Dimensional Mechanistic Model of *Prorocentrum Minimum* Blooms in Eutrophic Chesapeake bay. *Sci. Tot. Environ.* 769, 144528. doi: 10.1016/j.scitotenv.2020.144528

Zhong, L., and Li, M. (2006). Tidal Energy Fluxes and Dissipation in the Chesapeake bay. *Cont. Shelf. Res.* 26, 752–770. doi: 10.1016/j.csr.2006.02.006

Zhong, L., Li, M., and Foreman, M. G. (2008). Resonance and Sea Level Variability in Chesapeake bay. *Cont. Shelf. Res.* 28, 2565–2573. doi: 10.1016/j.csr.2008.07.007